

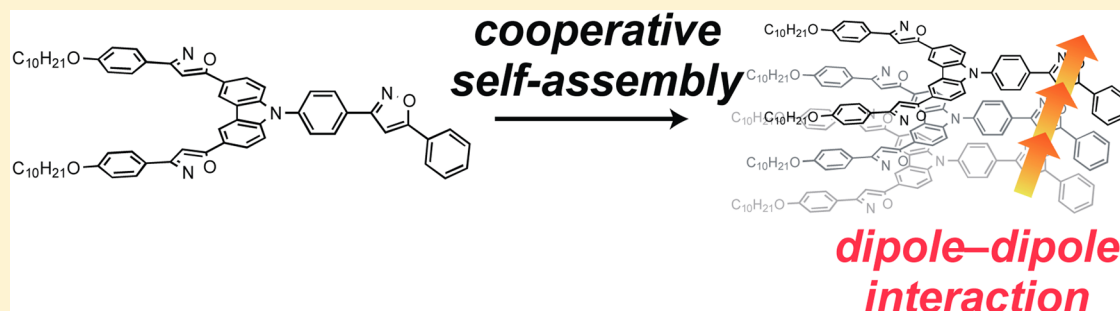
Cooperative Self-Assembly of Carbazole Derivatives Driven by Multiple Dipole–Dipole Interactions

Toshiaki Ikeda,[†] Tatsuya Iijima,[†] Ryo Sekiya,[†] Osamu Takahashi,[‡] and Takeharu Haino^{*,†}

[†]Department of Chemistry, Graduate School of Science, Hiroshima University, 1-3-1 Kagamiyama, Higashi-Hiroshima, 739-8526, Japan

[‡]Institute for Sustainable Sciences and Development, Hiroshima University, Higashi-Hiroshima 739-8526, Japan

S Supporting Information



ABSTRACT: Carbazole possessing phenylisoxazoles self-assembled in a cooperative manner in decalin. X-ray crystal structure analysis revealed that the isoxazole dipoles align in a head-to-tail fashion. DFT calculations suggested that the linear array of dipoles induced the polarization of each dipole, leading to an increase in dipole–dipole interactions. This dipole polarization resulted in cooperative assembly.

Precise regulation of the self-assembly of π -conjugated molecules is crucial for obtaining well-defined functional nanostructures¹ that produce photochemical² and electrochemical³ materials, organogels,⁴ and liquid crystals.⁵ Two major regimes (i.e., noncooperative (isodesmic) and cooperative) exist in the self-assembly process. The noncooperative self-assembly of π -conjugated molecules is governed by a single equilibrium constant (K_i).⁶ In contrast, the cooperative assembly of π -conjugated molecules has received more attention because this type of assembly leads to precise structural regulation of supramolecular organization, resulting in well-defined polymeric assemblies with small polydispersity indices (PDI) that are similar to those obtained in living polymerization.⁷ In general, cooperative self-assembly involves two assembling processes (i.e., initial nucleation process and successive elongation process). Positive cooperativity results from the more favorable elongation process. A high degree of cooperativity results in supramolecular living polymerization.⁸

Cooperativity in self-assembly is often encountered in one-dimensional supramolecular polymeric organization via directional head-to-tail hydrogen bonding.⁹ The linear array of amide groups generates intermolecular head-to-tail hydrogen bonds, which are oriented along the axis of the supramolecular polymeric organization. Recent theoretical investigations of hydrogen-bonded polymeric organizations reported that the linear organization of the amide groups induced polarization of the amide dipole, which facilitated strong dipole–dipole interactions. Therefore, the hydrogen-bonding interactions

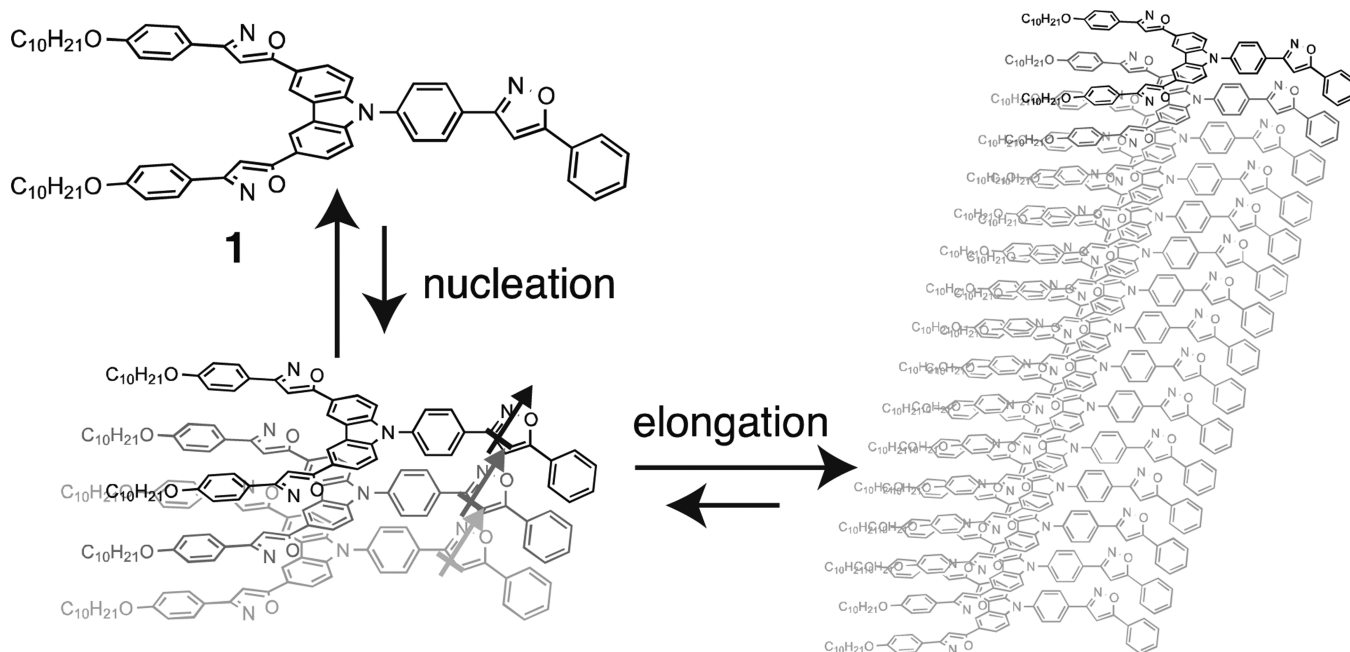
were greatly stabilized in the linear organization.¹⁰ Thus, most of the cooperative assemblies have been demonstrated in head-to-tail hydrogen-bonded supramolecular polymeric organizations. However, non-hydrogen-bonded supramolecular organizations rarely exhibit cooperative assemblies.¹¹

Our group has reported that planar π -conjugated molecules possessing phenylisoxazolyl moieties exhibit isodesmic assembly via π – π stacking and dipole–dipole interactions.¹² We envisioned that the perpendicular electronic interactions, which arise from the linear dipole arrays of isoxazolyl groups along the polymeric organization, can drive the cooperative assembly in our molecular stacks. In this context, carbazole derivative **1** possessing phenylisoxazoles was designed (Scheme 1). The two isoxazole rings adopt nearly coplanar arrangement relative to the carbazole ring, and the remaining isoxazole ring can be arranged in a nearly perpendicular conformation due to the per steric effect between the carbazole ring and the rotatable benzene ring. Therefore, the remaining isoxazole rings can be directionally aligned along the stacked polymeric organization. The self-assembly of **1** exhibited the cooperativity in decalin. The crystal structure of **1** revealed the linear organization of the dipole of the isoxazole rings that most likely directed the cooperative self-assembly in the polymeric organization.

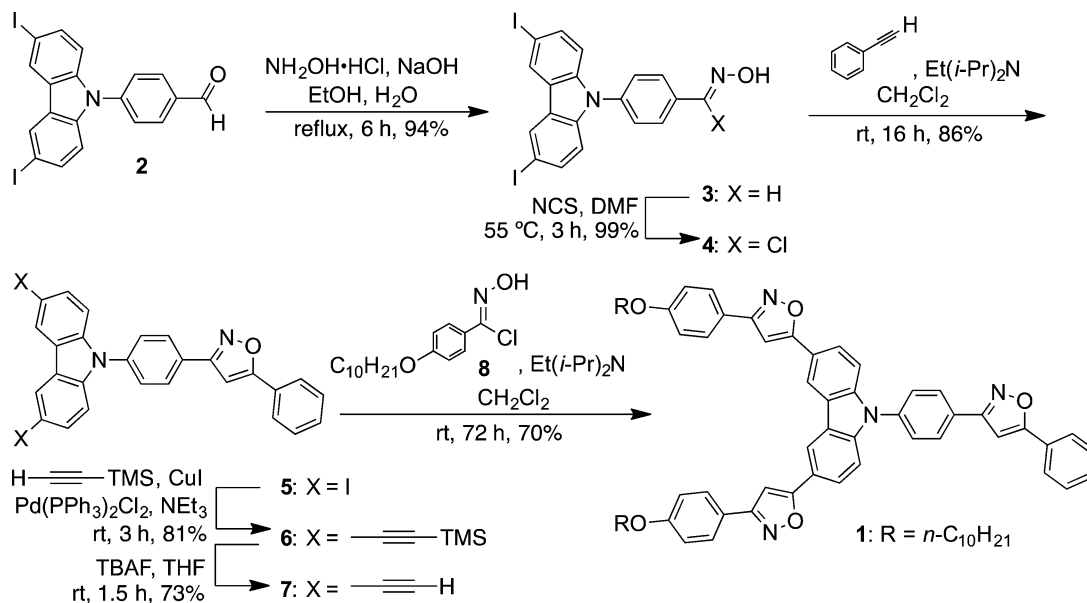
The synthesis of a carbazole derivative possessing three phenylisoxazoles **1** was summarized in Scheme 2. N-(4-

Received: May 18, 2016

Published: July 8, 2016

Scheme 1. Molecular Structure of **1** and Schematic Representation of the Cooperative Self-Assembly of **1**^a

^aArrows indicate the dipole moment of isoxazole rings.

Scheme 2. Synthesis of a Carbazole Derivative Possessing Phenylisoxazoles **1**

Formylphenyl)carbazole derivative **2** was converted to oxime **3**, which reacted with NCS to give chlorooxime **4**. 1,3-Dipolar cycloaddition reaction of **4** with phenylacetylene afforded *N*-(phenylisoxazolylphenyl)carbazole derivative **5**. TMS-acetylene was introduced to **5** by Sonogashira coupling to give **6**, then TMS groups were removed. 1,3-Dipolar cycloaddition reaction of **7** with chlorooxime **8** afforded the desired compound **1**.

The self-assembling behavior of **1** in chloroform-*d* was studied using NMR spectroscopy. The ¹H NMR signals of **1** were concentration dependent (Figure 1). Most of the aromatic signals were shifted upfield as the concentrations increased from 0.1 to 10.0 mmol L⁻¹. This result suggests that these molecules form stacked assemblies in which the aromatic protons are located in the shielding regions produced by the

neighboring molecules. Plotting the chemical shift changes of the protons as a function of the concentrations of **1** produced hyperbolic curves. Nonlinear curve-fitting analysis using an isodesmic model produced estimated complexation-induced shifts ($\Delta\delta = -0.11, -0.12, -0.22, -0.36, -0.24, -0.24, -0.23, -0.14, -0.08,$ and -0.11 ppm for H_a, H_b, H_c, H_d, H_e, H_f, H_g, H_h, H_i, and H_j, respectively) and an association constant (K_1) of 33 ± 6 L mol⁻¹ with a high probability (χ^2) of 0.997 (Figure S2). Therefore, **1** self-assembled in an isodesmic manner in chloroform-*d* at 25 °C. Aromatic protons H_c–H_g shifted more than the other protons, indicating that **1** stacked as piles around the carbazole.

To obtain more insight into the self-assembling behavior of **1**, UV–vis absorption spectroscopy was employed. **1** exhibited

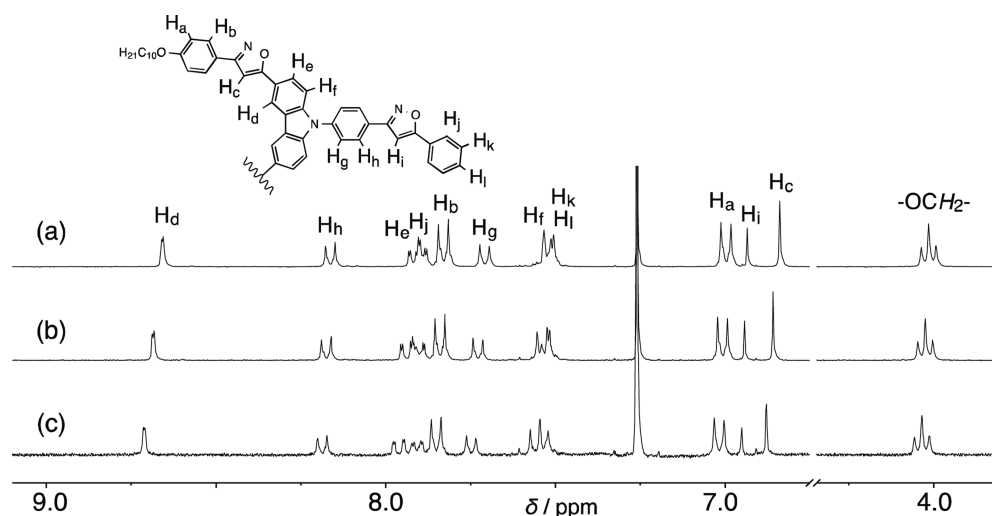


Figure 1. Concentration-dependent ^1H NMR spectra of **1** in chloroform-*d* at 25 °C. The concentrations are (a) 10.0, (b) 5.0, and (c) 1.0 mmol L $^{-1}$.

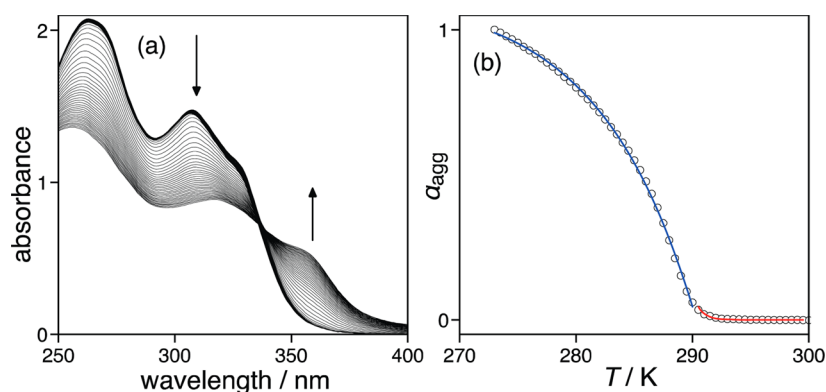


Figure 2. (a) Temperature-dependent UV-vis absorption spectra of **1** in decalin. The spectra were recorded every 0.5 °C. The arrows indicate the change in the spectra as the temperature decreased from 50 to 0 °C. $[\mathbf{1}] = 3.0 \times 10^{-5}$ mol L $^{-1}$. (b) Plot of the degree of aggregation (α_{agg}) at 360 nm as a function of temperature. Solid lines exhibit the fitting curve.

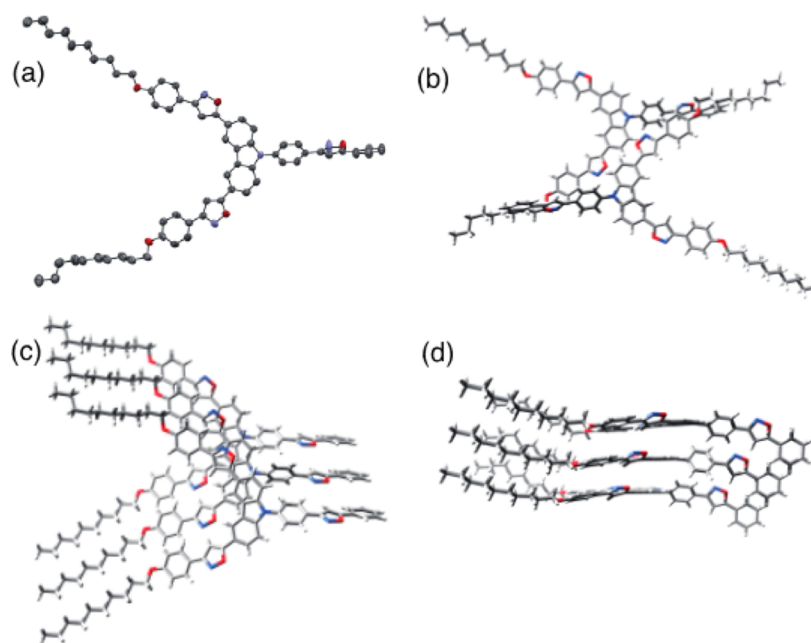


Figure 3. X-ray crystal structure of **1**. (a) Top view and (b–d) packing structure. (a) Hydrogen atoms were omitted for clarity.

absorption bands (269 and 309 nm) that were assigned to a monomeric carbazole in chloroform (Figure S5), indicating that **1** primarily exists in a monomeric form under these conditions. Employing decalin as a less-polar solvent results in the assembly of **1**. The UV-vis absorption spectra of **1** in decalin were temperature dependent. **1** exhibited monomeric absorption bands (266 and 310 nm) at 50 °C. However, the absorption bands decreased, and red-shifted bands (360 nm) emerged as the temperature decreased to 0 °C (Figures 2a and S6). These results suggest that **1** forms *J*-aggregates in decalin at low temperatures. It is important to note that the absorption spectra changed sharply at approximately 15 °C. The cooling curve for the degree of aggregation (α_{agg}) at 360 nm leads to a nonsigmoidal melting curve, which is characteristic of cooperative self-assembly (Figure 2b).

To gain thermodynamic insight into cooperative self-assembly, the cooling curve for α_{agg} of **1** based on absorption at 360 nm was analyzed by applying the van der Schoot mathematical model (Figure 2b).¹³ On the basis of the nonlinear least-squares analysis, the model provided a good description of the curve. The analysis provides an elongation temperature (T_e) of 290.28(4) K at the studied concentration, resulting in an association constant (K_e) of 3.3×10^4 L mol⁻¹ in the elongation process at T_e . The enthalpy release in the elongation process (ΔH_e) was $-88(2)$ kJ mol⁻¹, indicating that the elongation is an enthalpy-driven process. A dimensionless equilibrium constant (K_a) for the nucleation process to the elongation process was $1.20(9) \times 10^{-4}$. A higher degree of cooperativity is expressed by a smaller K_a value. Therefore, self-assembly of **1** exhibits fairly high cooperativity. The degree of polymerization at an elongation temperature ($N_n(T_e)$) of 20.2 was determined and is consistent with the size of the nucleus at the transition from the nucleation regime to the elongation regime.

The self-assembly of **1** is cooperative in decalin, whereas it is isodesmic in chloroform. The difference in the assembling behaviors might be rationalized by solvation. In our recent studies, π -conjugated molecules possessing phenylisoxazoles are well solvated in chloroform, which interferes with intermolecular association.^{12a,d,e,11d,12b} Therefore, the assemblies of **1** may not reach a certain size that enables the transition from the nucleation regime to the elongation regime.

The X-ray crystal structure analysis provides information on the assembly structure of **1** (Figures 3 and S8). X-ray quality crystals of **1** were obtained by slow evaporation of a chloroform solution of **1**. The phenylisoxazoles substituted at the 3- and 5-positions of the carbazole are nearly coplanar with the carbazole plane. However, the (phenylisoxazolyl)phenyl group that was substituted on the nitrogen of the carbazole was twisted to the carbazole plane due to the peri steric effect. The phenyl group attached to the nitrogen was disordered equally over two positions with dihedral angles (C–N–C–C) of 53.8 and -48.4° . The isoxazole ring was twisted with a dihedral angle of 68.6° to the carbazole plane. The unit cell contains two molecules of **1** in a face-to-face fashion (Figure 3b). The mean plane distance of the stacked carbazoles was 3.57 Å, which is consistent with the typical π – π stacking distance. The dipoles of the twisted isoxazole rings aligned along the stacking direction (Figure 3d). This result suggests that **1** assembled via intermolecular dipole–dipole interactions as well as π – π stacking interactions.

To understand the cooperativity in the self-assembly of **1**, density functional theory (DFT) calculations at the M06-2X/6-

31G(d,p) level were employed. The assembly structures of **1** up to a tetramer were extracted from the crystal structure, and the decyl side chains were displaced by methyl groups. Then, the total electronic energy (E_n) and the total dipole moment (D_n) were calculated at a single point without structure optimization. Basis set superposition error (BSSE) was corrected using the counter-poise method. **1** has two conformers in the crystal structure due to the disorder in the phenyl group attached to the nitrogen. Therefore, two conformations were calculated for each oligomer (see Figure S9). The results from the calculations are summarized in Table 1, where \bar{D}_n is the dipole

Table 1. Total Dipole Moment (D_n), Dipole Moment Per Molecule (\bar{D}_n), the Total Complexation Energy for the *n*-Mer (ΔE_n), and the Complexation Energy Per a Pair of Monomers ($\Delta \bar{E}_n$) Calculated Using DFT

<i>n</i> (conformation) ^a	D_n (Debye)	\bar{D}_n (Debye)	ΔE_n (kcal mol ⁻¹)	$\Delta \bar{E}_n$ (kcal mol ⁻¹)
1 (a)	4.2662	4.266		
1 (b)	4.3908	4.391		
2 (ab)	9.5436	4.772	-17.60	-17.6
2 (ba)	8.9438	4.472	-16.29	-16.3
3 (aba)	14.3855	4.795	-34.44	-17.2
3 (bab)	14.4747	4.825	-34.42	-17.2
4 (abab)	20.0866	5.022	-52.51	-17.5
4 (baba)	19.4245	4.856	-51.16	-17.1

^aConformations are shown in Figure S8.

moment per molecule ($\bar{D}_n = D_n/n$), ΔE_n indicates the total complexation energy for the *n*-mer, and $\Delta \bar{E}_n$ is the complexation energy per a pair of monomers ($\Delta \bar{E}_n = \Delta E_n/(n-1)$). All of the ΔE_n were negative, indicating that the assembly is favorable. \bar{D}_n of the oligomers is larger than that of the monomeric form. Growing the assemblies induces electronic polarization of the isoxazole ring, which results in enhancement of the dipole–dipole interactions. Therefore, an increase in the dipole–dipole interactions in the assembly most likely gives rise to the cooperativity of the assembly of **1**.¹⁴

In summary, we have demonstrated that carbazole **1** bearing phenylisoxazoles self-assembled in a cooperative manner in decalin. The dipoles of the isoxazole units that were oriented nearly perpendicular to the carbazole plane aligned in a head-to-tail fashion in the crystal structure. The results from DFT calculations of the oligomers revealed that the dipole moments per molecule increase as the oligomers grow. Therefore, intermolecular dipole–dipole interactions direct the cooperativity for the self-assembly of **1**.

EXPERIMENTAL SECTION

General. All reagents and solvents were of commercial reagent grade and were used without further purification except where noted. Dry CH₂Cl₂, DMF, and triethylamine were obtained by distillation over CaH₂. ¹H and ¹³C NMR spectra were recorded at 25 °C in CDCl₃ or in acetone-*d*₆, and chemical shifts were reported as the delta scale in ppm relative to CHCl₃ ($\delta = 7.26$ for ¹H and 77.3 for ¹³C) or acetone ($\delta = 2.09$ for ¹H and 30.6 (CH₃) for ¹³C). UV/vis absorption spectra in solution were measured using a conventional quartz cell (light path 1 cm) with temperature control. Preparative separations were performed by silica gel gravity column chromatography (Silica Gel 60N (spherical, neutral)). Compounds **2**¹⁵ and **8**^{12d} were prepared according to the reported methods.

3,6-Diiodo-N-(4-formylloximephenyl)carbazole (3). To a solution of **2** (8.00 g, 15.3 mmol) in ethanol (105 mL) was added sodium hydroxide (800 mg, 20.0 mmol) in water (2 mL) and hydroxylamine

hydrochloride (1.29 g, 18.6 mmol) in water (2 mL) at 0 °C. After allowing it to warm up to room temperature, the reaction mixture was stirred at reflux for 6 h under argon atmosphere. After the reaction mixture was filtered, the precipitate was washed by ethanol to give **3** (7.70 g, 94%) as a brown solid. Mp: 262–263 °C. ¹H NMR (300 MHz, acetone-*d*₆): δ 10.58 (s, 1H), 8.65 (d, *J* = 1.8 Hz, 2H), 8.31 (s, 1H), 7.95 (d, *J* = 8.4 Hz, 2H), 7.76 (dd, *J* = 1.8, 8.4 Hz, 2H), 7.66 (d, *J* = 8.4 Hz, 2H), and 7.29 (d, *J* = 8.4 Hz, 2H) ppm. ¹³C NMR (75 MHz, acetone-*d*₆): δ 147.6, 139.9, 137.2, 135.1, 133.2, 129.6, 128.3, 127.0, 124.6, 112.2, and 82.7 ppm. IR (KBr): ν 1605, 1519, 1467, 1427, 1361, 1313, 1280, 1228, 1168, 1108, 1051, 1017, 986, 935, 870, 836, 797, 633, 562, and 527 cm⁻¹. HRMS (ESI⁺) calcd for C₁₉H₁₃N₂O₁₂: *m/z* 538.9107 [M + H]⁺, found *m/z* 538.9112. Anal. Calcd for C₁₉H₁₂N₂O₁₂: C 42.41, H 2.25, N 5.21, found C 42.59, H 1.90, N 5.17%.

3,6-Diiodo-N-(4-formylchloroximephenyl)carbazole (4). To a solution of **3** (1.00 g, 1.86 mmol) in dry DMF (20 mL) at 0 °C was added *N*-chlorosuccinimide (280 mg, 2.10 mmol). After allowing it to warm up to room temperature, the reaction mixture was stirred at 55 °C for 3 h. The reaction mixture was poured into four volumes of water and extracted with AcOEt. The organic layer was washed with water five times, dried over sodium sulfate, and concentrated *in vacuo* to give **4** (1.06 g, 99%) as a brown solid. The product was used for the next reaction without further purification because of the lack of stability. ¹H NMR (300 MHz, CDCl₃): δ 8.39 (d, *J* = 1.8 Hz, 2H), 8.10 (d, *J* = 8.4 Hz, 2H), 7.86 (s, 1H), 7.68 (dd, *J* = 1.8, 8.7 Hz, 2H), 7.56 (d, *J* = 8.4 Hz, 2H), and 7.19 (d, *J* = 8.7 Hz, 2H) ppm.

3,6-Diiodo-N-(4-(3-phenylisoxazolyl)phenyl)carbazole (5). To a solution of **4** (1.06 g, 1.85 mmol) and phenylacetylene (2.5 mL, 22.8 mmol) in dry CH₂Cl₂ (20 mL) was added di-*iso*-propylethylamine (4.0 mL, 22.9 mmol). After being stirred at room temperature for 16 h, the reaction mixture was concentrated *in vacuo*. The crude product was purified by column chromatography on silica gel (AcOEt/hexane) to give **5** (1.02 g, 86%) as a white solid. Mp: 262–263 °C. ¹H NMR (300 MHz, CDCl₃): δ 8.41 (d, *J* = 1.5 Hz, 2H), 8.12 (d, *J* = 8.4 Hz, 2H), 7.89 (dd, *J* = 1.8, 8.4 Hz, 2H), 7.70 (dd, *J* = 1.8, 8.7 Hz, 2H), 7.63 (d, *J* = 8.4 Hz, 2H), 7.53–7.50 (m, 3H), 7.22 (d, *J* = 8.4 Hz, 2H), and 6.91 (s, 1H) ppm. ¹³C NMR (75 MHz, CDCl₃): δ 171.1, 162.2, 139.9, 138.3, 135.2, 134.3, 130.6, 129.6, 129.2, 128.7, 127.4, 126.0, 124.7, 112.0, 107.7, 97.5, and 83.4 ppm. IR (KBr): ν 1606, 1529, 1493, 1467, 1430, 1388, 1359, 1314, 1280, 1226, 1016, 950, 867, 799, 760, 688, 632, 565, and 418 cm⁻¹. HRMS (ESI⁺) calcd for C₂₇H₁₇N₂O₁₂: *m/z* 638.9425 [M + H]⁺, found *m/z* 638.9432. Anal. Calcd for C₂₇H₁₆N₂O₁₂: C 50.81, H 2.53, N 4.39, found C 50.59, H 2.53, N 4.47%.

3,6-Bis(trimethylsilylethynyl)-N-(4-(3-phenylisoxazolyl)phenyl)carbazole (6). To a stirred solution of **5** (1.02 g, 1.60 mmol) in dry triethylamine (25 mL) was added copper(I) iodide (15.2 mg, 0.08 mmol) under argon atmosphere. After stirring for 15 min, dichlorobis-(triphenylphosphine)palladium(II) (56 mg, 0.08 mmol) and trimethylsilylacetylene (2.3 mL, 16.4 mmol) were added sequentially to the reaction mixture. After stirring for 3 h at room temperature in the dark, the resulting mixture was poured into saturated aqueous ammonium chloride and extracted with ethyl acetate. The organic layer was washed with brine, dried over sodium sulfate, and concentrated *in vacuo*. The crude product was purified by column chromatography on silica gel (AcOEt/hexane) to give **6** (755 mg, 81%) as a white solid. Mp: 196–199 °C. ¹H NMR (300 MHz, CDCl₃): δ 8.25 (d, 1.2 Hz, 2H), 8.12 (d, *J* = 8.1 Hz, 2H), 7.89 (dd, *J* = 1.2, 8.7 Hz, 2H), 7.67 (d, *J* = 8.1 Hz, 2H), 7.56–7.51 (m, 5H), 7.36 (d, *J* = 8.7 Hz, 2H), 6.92 (s, 1H), and 0.30 (s, 18H) ppm. ¹³C NMR (75 MHz, CDCl₃): δ 171.1, 162.3, 140.8, 138.5, 130.6, 130.6, 129.3, 128.9, 128.7, 127.5, 127.4, 126.1, 124.8, 123.1, 115.4, 110.0, 106.1, 97.6, 92.8, and 0.3 ppm. IR (KBr): ν 2958, 2151, 1610, 1531, 1498, 1451, 1431, 1388, 1362, 1280, 1249, 1154, 952, 916, 860, 842, 762, 664, and 593 cm⁻¹. HRMS (ESI⁺) calcd for C₃₇H₃₄N₂OSi₂: *m/z* 601.2097 [M + Na]⁺, found *m/z* 601.2102. Anal. Calcd for C₃₇H₃₄N₂O₁₂: C 76.77, H 5.92, N 4.84, found C 76.53, H 5.99, N 4.86%.

3,6-Diethynyl-N-(4-(3-phenylisoxazolyl)phenyl)carbazole (7). To a stirred solution of **6** (755 mg, 1.30 mmol) in dry THF (40 mL) was

added tetra-*n*-butylammonium fluoride (2.50 g, 6.92 mmol), and the reaction mixture was stirred at room temperature for 1.5 h under argon atmosphere. The reaction mixture was concentrated *in vacuo* and extracted with ethyl acetate. The organic layer was washed with aqueous ammonium chloride, aqueous sodium bicarbonate, and brine, dried over sodium sulfate, and concentrated *in vacuo*. The crude product was purified by column chromatography on silica gel (AcOEt/hexane) to give **7** (413 mg, 73%) as a white solid. Mp: > 300 °C. ¹H NMR (300 MHz, CDCl₃): δ 8.27 (d, *J* = 1.8 Hz, 2H), 8.13 (d, *J* = 8.4 Hz, 2H), 7.89 (dd, *J* = 1.8, 8.1 Hz, 2H), 7.66 (d, *J* = 8.4 Hz, 2H), 7.58 (dd, *J* = 1.8, 8.4 Hz, 2H), 7.54–7.50 (m, 3H), 7.38 (d, *J* = 8.7 Hz, 2H), 6.91 (s, 1H), and 3.11 (s, 2H) ppm. ¹³C NMR (75 MHz, CDCl₃): δ 170.9, 162.0, 140.8, 138.2, 130.6, 130.5, 129.1, 128.8, 128.5, 127.3, 125.9, 124.7, 122.9, 114.2, 110.0, 97.3, 84.4, and 75.9 ppm. IR (KBr): ν 3308, 3277, 2105, 1611, 1572, 1532, 1478, 1450, 1432, 1389, 1367, 1284, 1240, 950, 810, 763, 685, 655, 611, and 589 cm⁻¹. HRMS (ESI⁺) calcd for C₃₁H₁₉N₂O: *m/z* 435.1492 [M + H]⁺, found *m/z* 435.1482. Anal. Calcd for C₃₁H₁₈N₂O•(H₂O)_{1.5}: C 80.68, H 4.59, N 6.07, found C 80.83, H 4.57, N 5.73%.

3,6-Bis(3-(4-decyloxyphenyl)isoxazolyl)-N-(4-(3-phenylisoxazolyl)phenyl)carbazole (1). To a solution of **7** (50 mg, 0.12 mmol) and **8** (117 mg, 0.37 mmol) in dry CH₂Cl₂ (3 mL) was added di-*iso*-propylethylamine (0.4 mL, 2.29 mmol). After stirring at room temperature for 72 h under argon atmosphere, the reaction mixture was concentrated *in vacuo* and extracted with ethyl acetate. The organic layer was washed with 1 N hydrochloric acid, aqueous sodium bicarbonate, and brine, dried over sodium sulfate, and concentrated *in vacuo*. The crude product was purified by preparative GPC-HPLC (chloroform) to give **1** (80 mg, 70%) as a white solid. Mp: 238–239 °C. ¹H NMR (300 MHz, CDCl₃): δ 8.68 (s, 2H), 8.17 (d, *J* = 8.1 Hz, 2H), 7.93 (d, *J* = 8.1 Hz, 2H), 7.90 (d, *J* = 7.8 Hz, 2H), 7.84 (d, *J* = 8.4 Hz, 4H), 7.73 (d, *J* = 7.8 Hz, 2H), 7.56–7.50 (m, 5H), 7.01 (d, *J* = 7.8 Hz, 4H), 6.94 (s, 1H), 6.86 (s, 2H), 4.02 (t, *J* = 6.6 Hz, 4H), 1.82 (quint, *J* = 6.6 Hz, 4H), 1.48 (m, 4H), 1.40–1.20 (m, 24H), and 0.89 (t, *J* = 6.6 Hz, 6H) ppm. ¹³C NMR (125 MHz, CDCl₃): δ 171.1, 170.7, 162.9, 162.1, 160.7, 142.0, 138.2, 130.6, 129.2, 129.2, 128.8, 128.3, 127.5, 127.4, 126.0, 124.9, 123.8, 121.6, 120.8, 118.6, 115.0, 110.7, 97.5, 96.6, 68.3, 32.0, 29.7, 29.7, 29.5, 29.4, 29.3, 26.1, 22.8, and 14.2 ppm. IR (KBr): ν 2923, 2851, 1610, 1528, 1493, 1471, 1436, 1390, 1362, 1333, 1292, 1255, 1231, 1176, 1022, 950, 834, 765, 688, and 651 cm⁻¹. HRMS (ESI⁺) calcd for C₆₅H₆₉N₄O₅: *m/z* 985.5263 [M + H]⁺, found *m/z* 985.5269. Anal. Calcd for C₆₅H₆₈N₄O₅•(H₂O)_{0.5}: C 78.52, H 7.00, N 5.63, found C 78.73, H 7.14, N 5.57%.

■ ASSOCIATED CONTENT

Supporting Information

The Supporting Information is available free of charge on the ACS Publications website at DOI: 10.1021/acs.joc.6b01169.

NMR and UV–vis absorption spectra, computational details, and ¹H and ¹³C NMR spectra of new synthesized compounds (PDF)

Crystallographic data for **1** (CIF)

■ AUTHOR INFORMATION

Corresponding Author

*Tel: +81-82-424-7427. Fax: +81-82-424-0724. E-mail: haino@hiroshima-u.ac.jp.

Notes

The authors declare no competing financial interest.

■ ACKNOWLEDGMENTS

This work was financially supported by Grant-in-Aid for Scientific Research (B), (C) (JP15H00752, JP15KT0145) and for Young Scientists (B) (JP26810051) of JSPS and Grant-in-Aid for Scientific Research in Innovative Areas: “Stimuli-responsive Chemical Species for the Creation of Functional

Molecules” and “New Polymeric Materials Based on Element-Blocks” (Nos. JP15H00946, JP15H00752) of MEXT.

REFERENCES

- (1) (a) Hoeben, F. J. M.; Jonkheijm, P.; Meijer, E. W.; Schenning, A. P. H. *J. Chem. Rev.* **2005**, *105*, 1491–1546. (b) Palmer, L. C.; Stupp, S. I. *Acc. Chem. Res.* **2008**, *41*, 1674–1684. (c) Zang, L.; Che, Y.; Moore, J. S. *Acc. Chem. Res.* **2008**, *41*, 1596–1608. (d) Pisula, W.; Feng, X.; Müllen, K. *Adv. Mater.* **2010**, *22*, 3634–3649. (e) Aida, T.; Meijer, E. W.; Stupp, S. I. *Science* **2012**, *335*, 813–817.
- (2) (a) Würthner, F. *Chem. Commun.* **2004**, 1564–1579. (b) Elemans, J. A. A. W.; Van Hameren, R.; Nolte, R. J. M.; Rowan, A. E. *Adv. Mater.* **2006**, *18*, 1251–1266. (c) Wasielewski, M. R. *Acc. Chem. Res.* **2009**, *42*, 1910–1921. (d) Würthner, F.; Kaiser, T. E.; Saha-Möllner, C. R. *Angew. Chem., Int. Ed.* **2011**, *50*, 3376–3410.
- (3) (a) Schenning, A. P. H. J.; Meijer, E. W. *Chem. Commun.* **2005**, 3245–3258. (b) Nguyen, T.-Q.; Martel, R.; Bushey, M.; Avouris, P.; Carlsen, A.; Nuckolls, C.; Brus, L. *Phys. Chem. Chem. Phys.* **2007**, *9*, 1515–1532. (c) Beaujuge, P. M.; Fréchet, J. M. J. *J. Am. Chem. Soc.* **2011**, *133*, 20009–20029. (d) Li, H.; Choi, J.; Nakanishi, T. *Langmuir* **2013**, *29*, 5394–5406.
- (4) (a) Ishi-i, T.; Shinkai, S. *Top. Curr. Chem.* **2005**, *258*, 119–160. (b) Ajayaghosh, A.; Praveen, V. K. *Acc. Chem. Res.* **2007**, *40*, 644–656. (c) Babu, S. S.; Praveen, V. K.; Ajayaghosh, A. *Chem. Rev.* **2014**, *114*, 1973–2129.
- (5) (a) Laschat, S.; Baro, A.; Steinke, N.; Giesselmann, F.; Hägele, C.; Scalia, G.; Judele, R.; Kapatsina, E.; Sauer, S.; Schreivogel, A.; Tosoni, M. *Angew. Chem., Int. Ed.* **2007**, *46*, 4832–4887. (b) Sergeev, S.; Pisula, W.; Geerts, Y. H. *Chem. Soc. Rev.* **2007**, *36*, 1902–1929. (c) Kato, T.; Yasuda, T.; Kamikawa, Y.; Yoshio, M. *Chem. Commun.* **2009**, 729–739. (d) Pisula, W.; Zorn, M.; Chang, J. Y.; Müllen, K.; Zentel, R. *Macromol. Rapid Commun.* **2009**, *30*, 1179–1202.
- (6) (a) Martin, R. B. *Chem. Rev.* **1996**, *96*, 3043–3064. (b) De Greef, T. F. A.; Smulders, M. M. J.; Wolfs, M.; Schenning, A. P. H. J.; Sijbesma, R. P.; Meijer, E. W. *Chem. Rev.* **2009**, *109*, 5687–5754. (c) Smulders, M. M. J.; Nieuwenhuizen, M. M. L.; de Greef, T. F. A.; van der Schoot, P.; Schenning, A. P. H. J.; Meijer, E. W. *Chem. - Eur. J.* **2010**, *16*, 362–367.
- (7) (a) van Gestel, J.; van der Schoot, P.; Michels, M. A. J. *J. Phys. Chem. B* **2001**, *105*, 10691–10699. (b) Zhao, D.; Moore, J. S. *Org. Biomol. Chem.* **2003**, *1*, 3471–3491. (c) Markvoort, A. J.; ten Eikelder, H. M. M.; Hilbers, P. A. J.; de Greef, T. F. A.; Meijer, E. W. *Nat. Commun.* **2011**, *2*, 509. (d) van der Zwaag, D.; Pieters, P. A.; Korevaar, P. A.; Markvoort, A. J.; Spiering, A. J. H.; de Greef, T. F. A.; Meijer, E. W. *J. Am. Chem. Soc.* **2015**, *137*, 12677–12688.
- (8) (a) Ogi, S.; Fukui, T.; Jue, M. L.; Takeuchi, M.; Sugiyasu, K. *Angew. Chem., Int. Ed.* **2014**, *53*, 14363–14367. (b) Ogi, S.; Sugiyasu, K.; Manna, S.; Samitsu, S.; Takeuchi, M. *Nat. Chem.* **2014**, *6*, 188–195. (c) Kang, J.; Miyajima, D.; Mori, T.; Inoue, Y.; Itoh, Y.; Aida, T. *Science* **2015**, *347*, 646–651. (d) Ogi, S.; Stepanenko, V.; Sugiyasu, K.; Takeuchi, M.; Würthner, F. *J. Am. Chem. Soc.* **2015**, *137*, 3300–3307.
- (9) (a) Jonkheijm, P.; van der Schoot, P.; Schenning, A. P. H. J.; Meijer, E. W. *Science* **2006**, *313*, 80–83. (b) Gopal, A.; Hifsudheen, M.; Furumi, S.; Takeuchi, M.; Ajayaghosh, A. *Angew. Chem., Int. Ed.* **2012**, *51*, 10505–10509. (c) García, F.; Korevaar, P. A.; Verlee, A.; Meijer, E. W.; Palmans, A. R. A.; Sánchez, L. *Chem. Commun.* **2013**, *49*, 8674–8676.
- (10) (a) Kobko, N.; Paraskevas, L.; del Rio, E.; Dannenberg, J. J. *J. Am. Chem. Soc.* **2001**, *123*, 4348–4349. (b) Kobko, N.; Dannenberg, J. J. *J. Phys. Chem. A* **2003**, *107*, 10389–10395. (c) Filot, I. A. W.; Palmans, A. R. A.; Hilbers, P. A. J.; van Santen, R. A.; Pidko, E. A.; de Greef, T. F. A. *J. Phys. Chem. B* **2010**, *114*, 13667–13674.
- (11) (a) Fernández, G.; Stolte, M.; Stepanenko, V.; Würthner, F. *Chem. - Eur. J.* **2013**, *19*, 206–217. (b) Mayoral, M. J.; Rest, C.; Stepanenko, V.; Schellheimer, J.; Albuquerque, R. Q.; Fernández, G. *J. Am. Chem. Soc.* **2013**, *135*, 2148–2151. (c) Tian, Y.-J.; Meijer, E. W.; Wang, F. *Chem. Commun.* **2013**, *49*, 9197–9199. (d) Ikeda, T.; Takayama, M.; Kumar, J.; Kawai, T.; Haino, T. *Dalton Trans.* **2015**, *44*, 13156–13162.
- (12) (a) Haino, T.; Tanaka, M.; Fukazawa, Y. *Chem. Commun.* **2008**, 468–470. (b) Haino, T.; Saito, H. *Synth. Met.* **2009**, *159*, 821–826. (c) Haino, T.; Saito, H. *Aust. J. Chem.* **2010**, *63*, 640–645. (d) Tanaka, M.; Ikeda, T.; Mack, J.; Kobayashi, N.; Haino, T. *J. Org. Chem.* **2011**, *76*, 5082–5091. (e) Ikeda, T.; Masuda, T.; Hirao, T.; Yuasa, J.; Tsumatori, H.; Kawai, T.; Haino, T. *Chem. Commun.* **2012**, *48*, 6025–6027. (f) Haino, T.; Hirai, Y.; Ikeda, T.; Saito, H. *Org. Biomol. Chem.* **2013**, *11*, 4164–4170. (g) Haino, T.; Ueda, Y.; Hirao, T.; Ikeda, T.; Tanaka, M. *Chem. Lett.* **2014**, *43*, 414–416. (h) Ikeda, T.; Masuda, T.; Takayama, M.; Adachi, H.; Haino, T. *Org. Biomol. Chem.* **2016**, *14*, 36–39.
- (13) (a) *Supramolecular Polymers*, 2nd ed.; Ciferri, A., Ed.; CRC Press-Taylor & Francis: Boca Raton, FL, 2005. (b) Smulders, M. M. J.; Schenning, A. P. H. J.; Meijer, E. W. *J. Am. Chem. Soc.* **2008**, *130*, 606–611.
- (14) We carried out the energy decomposition analysis in 2mer-ab (Table S2). The results indicate that the electrostatic energy is dominant in the intermolecular interactions, which represents the intermolecular dipole–dipole interaction.
- (15) Teng, C.; Yang, X. C.; Li, S. F.; Cheng, M.; Hagfeldt, A.; Wu, L. Z.; Sun, L. C. *Chem. - Eur. J.* **2010**, *16*, 13127–13138.